Sec16 function in ER export and autophagy is independent of its phosphorylation in *Saccharomyces cerevisiae*

Tomohiro Yorimitsu and Ken Sato*
Department of Life Sciences, Graduate School of Arts and Sciences, University of Tokyo, Tokyo 153-8902, Japan

ABSTRACT **Coat protein complex II (COPII) protein assembles at the endoplasmic reticulum exit site (ERES) to form vesicle carrier for transport from the ER to the Golgi apparatus. Sec16 has a critical role in COPII assembly to form ERES. Sec16$^{\Delta 565N}$ mutant, which lacks the N-terminal 565 amino acids, is defective in ERES formation and ER export. Several phosphoproteomic studies have identified 108 phosphorylated Ser/Thr/Tyr residues in Sec16 of *Saccharomyces cerevisiae*, of which 30 residues are located in the truncated part of Sec16$^{\Delta 565N}$. The exact role of the phosphorylation in Sec16 function remains to be determined. Therefore, we analyzed nonphosphorylatable Sec16 mutants, in which all identified phosphorylation sites are substituted with Ala. These mutants show ERES and ER export comparable to those of wild-type Sec16, although the nonphosphorylatable mutant binds the COPII subunit Sec23 more efficiently than the wild-type protein. Because nutrient starvation–induced autophagy depends on Sec16, Sec16$^{\Delta 565N}$ impairs autophagy, whereas the nonphosphorylatable mutants do not affect autophagy. We conclude that Sec16 phosphorylation is not essential for its function.**

Monitoring Editor
Akihiko Nakano
RIKEN

Received: Sep 4, 2019
Revised: Nov 27, 2019
Accepted: Dec 12, 2019

INTRODUCTION

The intracellular transport starts at the endoplasmic reticulum (ER). The coat protein complex II (COPII) machineries mediate the formation of transport vesicles from the ER. Extensive studies have revealed the processes involved in COPII vesicle formation. ER-resident Sec12 activates the small GTPase Sar1 by catalyzing its GTP binding, which allows Sar1 to relocate to the ER membrane (Nakano and Muramatsu, 1989; Barlowe and Schekman, 1993). The inner coat Sec23/Sec24 complex is recruited to membrane-bound Sar1, followed by recruitment of the outer coat Sec13/Sec31 complex, which deforms the membranes followed by sculpting COPII vesicles (Matsuoka *et al.*, 1998; Bi *et al.*, 2002, 2007; Tabata *et al.*, 2009; Iwasaki *et al.*, 2017). Sec24 and its paralogues act as cargo adaptors to mediate incorporation of cargo proteins into nascent vesicles (Roberg *et al.*, 1999; Kurihara *et al.*, 2000; Miller *et al.*, 2002, 2003). Sec23 serves as a GTPase-activating protein (GAP) against Sar1, which is stimulated by Sec31, leading to removal of Sar1 from forming vesicles (Yoshihisa *et al.*, 1993; Antonny *et al.*, 2001).

COPII protein assembles at the specialized ER domain, the ER exit site (ERES). COPII vesicles loaded with specific cargoes is thought to exit from distinct ERESs (Castillon *et al.*, 2009; Iwasaki *et al.*, 2015). Inactivation of Sec16 impairs ERES formation and ER export (Connerly *et al.*, 2005; Shindiapina and Barlowe, 2010; Yorimitsu and Sato, 2012). Like other COPII components, Sec16 is conserved among species and has the structured central conserved domain (CCD) flanked by the unstructured N- and C-terminal regions (Whittle and Schwartz, 2010; Pietrosemoli *et al.*, 2013; Sprangers and Rabouille, 2015). Sec16 interacts with all COPII components through distinct regions (Gimeno *et al.*, 1995; Shaywitz *et al.*, 1997; Yorimitsu and Sato, 2012). Therefore, Sec16 acts as a scaffold for COPII assembly to form ERES (Barlowe and Miller, 2013; Lord *et al.*, 2013). Sec16 also regulates COPII functions in vesicle formation processes (Bharucha *et al.*, 2013). In vitro reconstitution experiments have shown that Sec16 inhibits Sec31-stimulated Sec23 activation by preventing Sec31 from binding to Sec23, which

This article was published online ahead of print in MBoC in Press (http://www.molbiolcell.org/cgi/doi/10.1091/mbc.E19-08-0477) on December 18, 2019.
The authors declare no competing interests.
*Address correspondence to: Ken Sato (kensato@bio.c.u-tokyo.ac.jp).
Abbreviations used: CCD, central conserved domain; COPII, coat protein complex II; CPY, carboxypeptidase Y; ER, endoplasmic reticulum; ERES, ER exit site; PAS, preautophagosomal structure.

may stabilize COPII assembly (Kung *et al.*, 2012; Yorimitsu and Sato, 2012).

COPII proteins are regulated by phosphorylation. Sec23 is shown to be phosphorylated, and its phosphorylation is suggested to be involved in the uncoating process (Lord *et al.*, 2011). Under nutrient starvation conditions, Sec23 and Sec24 also undergo phosphorylation to serve in autophagy (Davis *et al.*, 2016; Gan *et al.*, 2017). Autophagy is a degradation process in the vacuole/lysosome. When nutrient starvation triggers autophagy, a membrane structure called the autophagosome emerges at preautophagosomal structure (PAS), where autophagy-related (Atg) proteins are assembled. It engulfs the cytoplasmic materials and delivers them to the vacuole/lysosome where they are digested and recycled for survival (Nakatogawa *et al.*, 2009; Feng *et al.*, 2014). Mounting evidence has currently demonstrated the connection between autophagy and a COPII system (Davis *et al.*, 2017; Zahoor and Farhan, 2018). The PAS has been shown to contact the ERES, which is suggested to directly transfer lipid molecules from the ER to forming autophagosomes (Graef *et al.*, 2013; Suzuki *et al.*, 2013; Kotani *et al.*, 2018). Recent work has also revealed that COPII vesicles are directly targeted to autophagosomes to supply the membrane source (Shima *et al.*, 2019). Autophagy induction is proposed to trigger COPII vesicles directing to the Golgi to be redirected to autophagosomes (Lemus *et al.*, 2016). In this model, Sec24 phosphorylation is a key event to promote Sec24 to interact with Atg9 and to mediate the redirection of vesicles (Davis *et al.*, 2016). Autophagy is known to require Sec16 (Ishihara *et al.*, 2001). However, current knowledge of the role of Sec16 in autophagy is limited.

Sec16 is also known to undergo phosphorylation. Two phosphorylation sites are mapped in the N-terminal region of mammalian homologue Sec16A (Farhan *et al.*, 2010; Joo *et al.*, 2016). In *Drosophila*, Sec16 is shown to be phosphorylated in the C-terminal region in response to nutrient starvation (Zacharogianni *et al.*, 2011). In *Saccharomyces cerevisiae* Sec16, several phosphoproteomic studies have so far identified 108 phosphorylated Ser/Thr/Tyr residues throughout the regions except for the CCD, and also revealed that some sites are responsive to starvation and treatment with the autophagy inducer rapamycin (Figure 1A and Supplemental

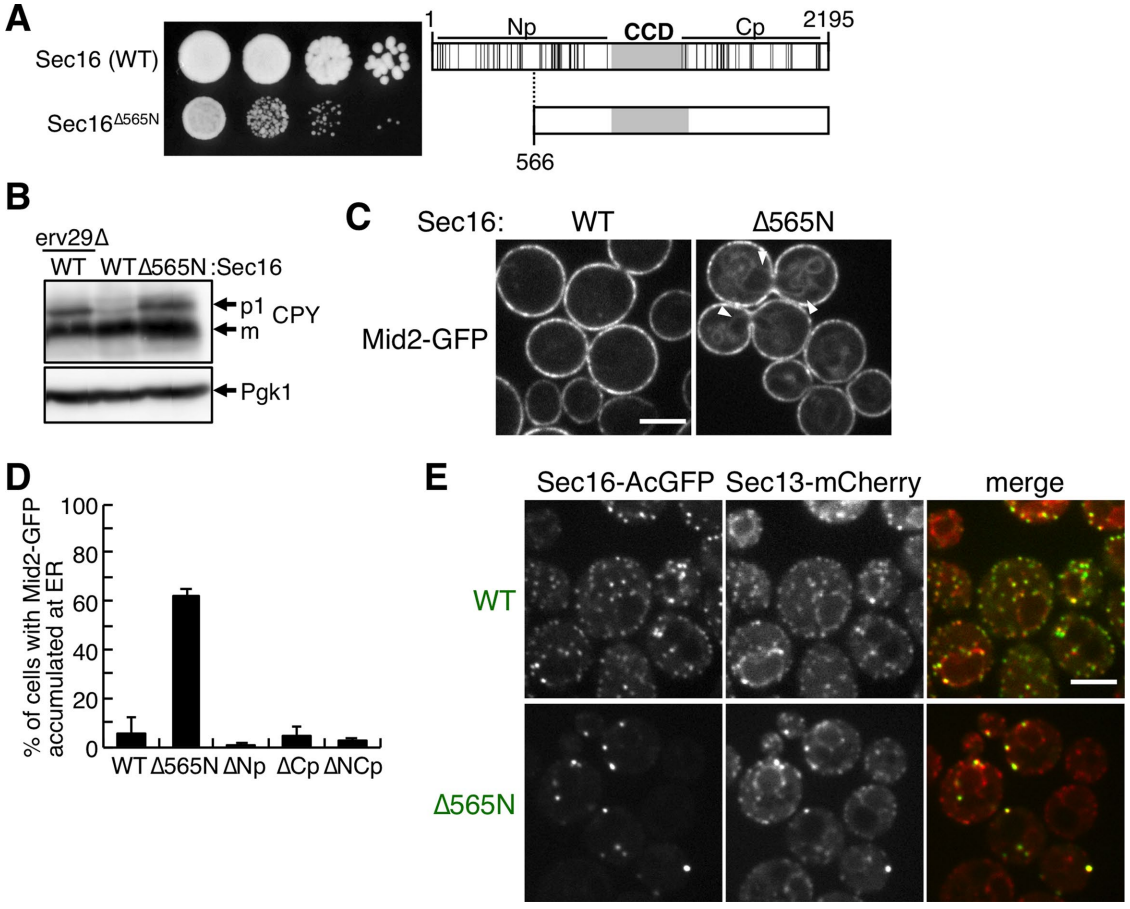

FIGURE 1: Sec16$^{\Delta 565N}$ mutant shows defects in ERES formation and ER export. (A) Tenfold serial dilutions of cultures of *sec16*Δ cells expressing wild-type Sec16 or Sec16$^{\Delta 565N}$ mutant were spotted on YPD plates and grown at 30°C for 2 d. The right panel is the schematic representation of wild-type Sec16 and Sec16$^{\Delta 565N}$ mutant. The gray box represents the CCD. Black lines in wild-type Sec16 represent locations of phosphorylation sites as shown in Supplemental Figure S1A. Np, 62 N-terminal phosphorylation sites; Cp, 46 C-terminal phosphorylation sites. (B) CPY transport was examined by immunoblotting in *erv29*Δ *sec16*Δ cells expressing wild-type Sec16, and *sec16*Δ cells expressing wild-type Sec16 or Sec16$^{\Delta 565N}$ mutant. (C) Mid2-GFP transport was monitored by fluorescence microscopy in *sec16*Δ cells expressing wild-type Sec16 or Sec16$^{\Delta 565N}$ mutant. Arrowheads indicate Mid2-GFP accumulated in the ER. Scale bars, 4 μm. (D) The percentage of cells showing Mid2-GFP accumulated in the ER. Error bars indicate the SD of three experiments. (E) *sec16*Δ cells expressing Sec16-AcGFP or Sec16$^{\Delta 565N}$-AcGFP with Sec13-mCherry were observed by fluorescence microscopy. Sec16 constructs visualized in the green channel are indicated in green. Scale bars, 4 μm.

Figure S1A; Albuquerque *et al.*, 2008; Holt *et al.*, 2009; Swaney *et al.*, 2013; Iesmantavicius *et al.*, 2014). It remains unclear whether the phosphorylation at any of these sites has a role in Sec16 function. Analysis of serial truncation mutants of Sec16 has previously shown that Sec16$^{\Delta 565N}$ mutant exhibits poor growth (Yorimitsu and Sato, 2012). This mutant lacks the region of the N-terminal 565 residues including the 30 phosphorylation sites. Whether loss of these phosphorylation sites is associated with the defects of Sec16$^{\Delta 565N}$ is not known.

In this study, we created nonphosphorylatable Sec16 mutants in which all 108 phosphorylation sites are substituted with Ala. We found that the nonphosphorylatable mutants display ERES, ER export, and autophagy comparable to those of wild-type Sec16. Surprisingly, our data indicate that Sec16 phosphorylation is not essential for its function.

RESULTS AND DISCUSSION

The N-terminal region of Sec16 is required for ERES formation and ER export

We set out to investigate the effect of Sec16$^{\Delta 565N}$ mutant on COPII-mediated transport. As shown in our previous complementation assay (Yorimitsu and Sato, 2012), when expressed as a sole copy of Sec16 in *sec16*Δ cells, Sec16$^{\Delta 565N}$ exhibited growth defect (Figure 1A). We next checked the ER–Golgi transport in *sec16*Δ cells expressing Sec16$^{\Delta 565N}$. Carboxypeptidase Y (CPY) is exported from the ER to the Golgi in a COPII-dependent manner, and then delivered to the vacuole, where it is processed to become the mature form. Because Erv29 acts as a cargo receptor to incorporate CPY efficiently into the COPII vesicle (Belden and Barlowe, 2001), the ER-specific p1 form of CPY is accumulated in *erv29*Δ background cells (Figure 1B). Similarly, Sec16$^{\Delta 565N}$ displayed significant accumulation of the p1 form. We also examined the distribution of Mid2-GFP by fluorescence microscopy (Figure 1, C and D). Mid2-GFP is exported as a COPII cargo protein from the ER, and finally localizes to the plasma membrane (Ono *et al.*, 1994), as observed in cells with wild-type Sec16. Sec16$^{\Delta 565N}$ showed Mid2-GFP localization to the plasma membrane but also its presence in the ER, indicating the accumulation of Mid2-GFP in the ER. Collectively, these results indicate that Sec16$^{\Delta 565N}$ reduced the efficiency of ER export.

Finally, we examined the distribution of Sec13-mCherry and Sec16-AcGFP by fluorescence microscopy in order to investigate ERES formation (Figure 1E). Although both Sec16-AcGFP and Sec16$^{\Delta 565N}$-AcGFP colocalized together with Sec13-mCherry, Sec16$^{\Delta 565N}$-AcGFP and Sec13-mCherry exhibited aberrantly exaggerated ERES, compared with a typical dispersed ERES pattern of Sec16-AcGFP. These results suggest that the N-terminal region lacking in Sec16$^{\Delta 565N}$ plays a critical role in the proper formation and/or organization of ERES.

Previous results have shown that Sec16$^{\Delta 565N}$ lacks the Sec31-binding site and is unable to interact with Sec31 (Kung *et al.*, 2012; Yorimitsu and Sato, 2012). Based on the results shown below, defects of Sec16$^{\Delta 565N}$ might be caused by loss of the ability to interact with Sec31. Sec16 mutant lacking the 60 amino acid residues for the Sec31 binding was previously shown to be defective in cell growth and CPY transport (Yorimitsu and Sato, 2012). This finding shed light on the implication of the Sec16-Sec31 interaction in ER export, although the underlying details remained unclear. Here, we provide a novel insight into the role of the Sec16-Sec31 interaction in organizing ERES formation to ensure typical dispersed ERESs throughout the ER. In *Pichia pastoris*, correct Sec16 localization at the ERES was shown to require the N-terminal region that binds Sec23, Sec24, and Sec31 (Bharucha *et al.*, 2013). In contrast to our observation, loss of this region abolished *P. pastoris* Sec16 from ERES. This different observation might come from the difference in the COPII proteins binding in the regions. Our previous pull-down analysis showed that the Sec31-binding site bound neither Sec23 nor Sec24 (Yorimitsu and Sato, 2012). Thus, our observation may reflect the exact effects of the interaction with Sec31 on Sec16 function.

Sec16 phosphorylation is dispensable for its function in ER export

Two distinct phosphorylation sites, Thr-415 and Ser-846, were identified in the N-terminal region of mammalian Sec16 homologue Sec16A (Farhan *et al.*, 2010; Joo *et al.*, 2016). Because the nonphosphorylatable Sec16A mutants of each of these residues affected the number of ERES, phosphorylation is suggested to be implicated in ERES formation. In *S. cerevisiae*, there are 108 phosphorylated Ser/Thr/Tyr residues identified in Sec16, of which the 30 residues exist in the N-terminal regions truncated in Sec16$^{\Delta 565N}$ (Figure 1A and Supplemental Figure S1A). This prompted us to wonder whether loss of these 30 phosphorylation sites would be associated with the defects of Sec16$^{\Delta 565N}$. It has been noted that two Sec16A phosphorylation sites appear not to be conserved in *S. cerevisiae* Sec16, due to a high divergence of Sec16 sequence among species (Joo *et al.*, 2016). Therefore, we created nonphosphorylatable mutant Sec16$^{\Delta NP}$ by substituting the 62 phosphorylation sites in the N-terminal region with Ala. Simultaneously, to extend our focus to the C-terminal phosphorylation sites, we created Sec16$^{\Delta CP}$ and Sec16$^{\Delta NCP}$ mutants with Ala substitutions of the C-terminal 46 sites, and the entire 108 sites, respectively.

Growth assay showed that each of these mutants could support viability in *sec16*Δ cells as well as wild-type Sec16 (Figure 2A). Consistently, the nonphosphorylatable mutant with substitutions in 30 phosphorylation sites did not show defect in cell growth (our unpublished data). Additionally, in contrast to *sec16*Δ cells expressing the temperature-sensitive mutant Sec16^{L1089P}, which grew at 23°C but not at 37°C, *sec16*Δ cells expressing the nonphosphorylatable mutants were not temperature-sensitive, and grew as well as those expressing wild-type Sec16 under both conditions (Supplemental Figure S1B). We then examined ER export in *sec16*Δ cells expressing the nonphosphorylatable mutants. These mutants did not exhibit significant accumulation of the p1 form of CPY comparable to that of the wild-type protein (Figure 2B). Fluorescence microscopy also revealed proper localization of Mid2-GFP to the plasma membrane but no accumulation in the ER with the nonphosphorylatable mutants (Figures 1C and 2C). These results indicate that unlike Sec16$^{\Delta 565N}$, the nonphosphorylatable mutants retain the ability to drive ER export.

We next investigated ERES formation by visualizing the mUkG1-fused nonphosphorylatable mutants along with Sec13-mCherry by fluorescence microscopy (Figure 2D). These mutants all displayed colocalization with Sec13-mCherry at ERES, comparable to that of wild-type Sec16-mUkG1, indicating proper formation of ERES. Collectively, these findings clearly rule out the possibility that loss of the N-terminal phosphorylation sites is the cause for the defects of Sec16$^{\Delta 565N}$.

The nonphosphorylatable Sec16 mutant shows increased interaction with Sec23

Finally, we immunoprecipitated HA-tagged Sec16 from detergent-solubilized cell lysates and checked the phosphorylation by immunoblotting using an antibody that recognizes phosphorylated Ser/Thr residues (Figure 3A). Phosphorylation was detected on

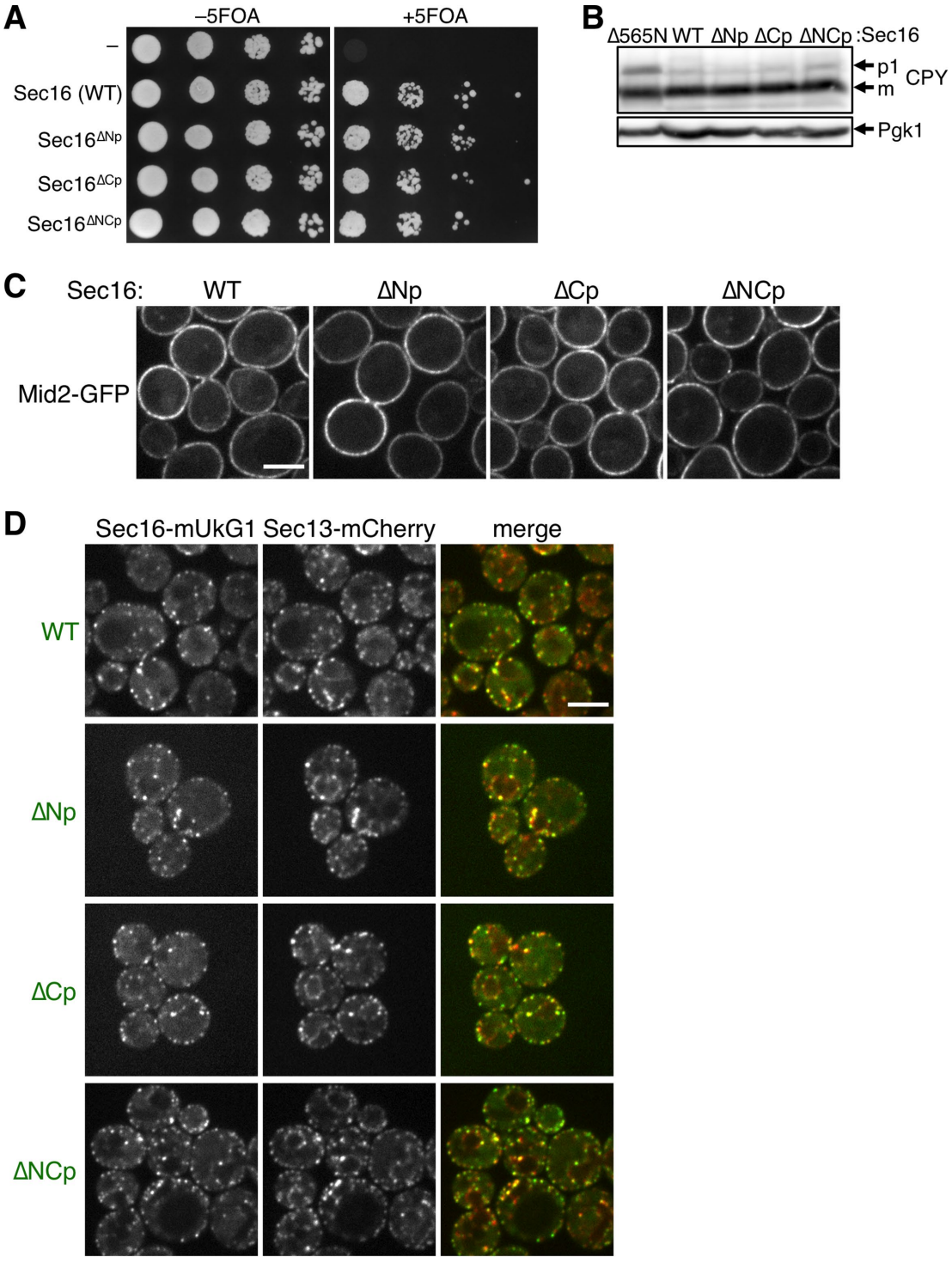

FIGURE 2: Nonphosphorylatable Sec16 mutants show normal ERES formation and ER export. (A) Tenfold serial dilutions of cultures of *sec16Δ* cells expressing Sec16 from a *URA3* plasmid along with an empty vector or a plasmid encoding wild-type Sec16 or the indicated Sec16 phosphomutants were spotted on plates in the presence or absence of 5-FOA and grown at 30°C for 3 d. (B) CPY transport was examined in *sec16Δ* cells expressing wild-type Sec16 or the indicated Sec16 mutants. (C) Mid2-GFP transport was monitored by fluorescence microscopy in *sec16Δ* cells expressing wild-type Sec16 or the indicated Sec16 mutants. Scale bars, 4 μm. (D) *sec16Δ* cells expressing mUkG1-fused wild-type Sec16 or nonphosphorylatable mutants with Sec13-mCherry were observed by fluorescence microscopy. Sec16 constructs visualized in the green channel are indicated in green. Scale bars, 4 μm.

immunoprecipitated Sec16-HA but not on Sec16$^{\Delta NCp}$-HA. We further analyzed these immunoprecipitates in order to examine an in vivo interaction between Sec16 and endogenous Sec23. Sec16 has the binding sites for Sec23 in the N-terminal and C-terminal regions (Espenshade *et al.*, 1995; Yorimitsu and Sato, 2012; Bharucha *et al.*, 2013), and these sites are phosphorylated. Therefore, we wondered

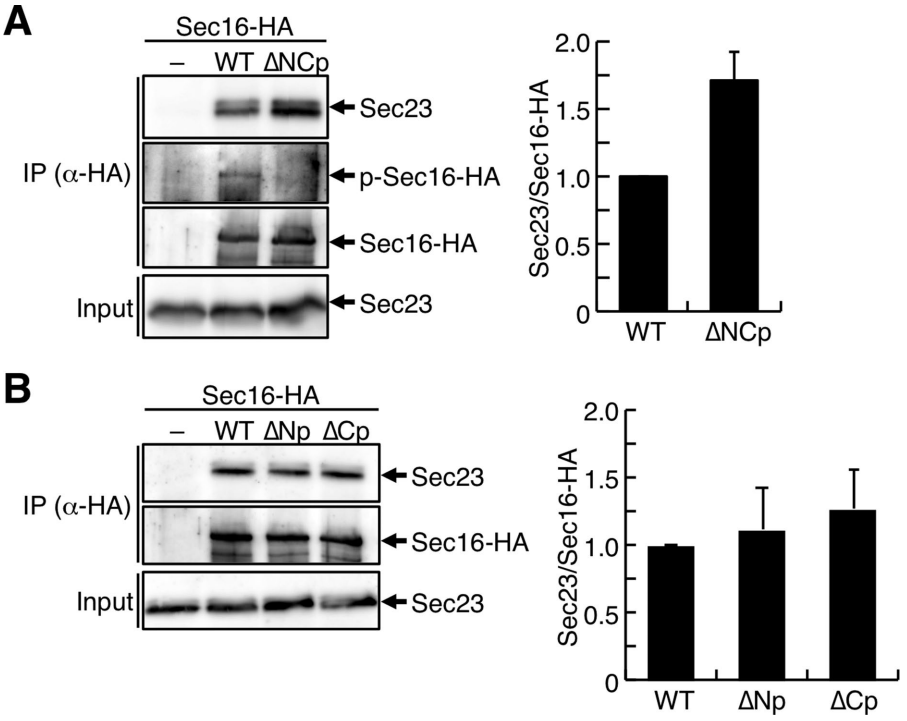

FIGURE 3: Sec16$^{\Delta NCp}$ mutant shows increased interaction with Sec23. (A) Sec16-HA and Sec16$^{\Delta NCp}$-HA were immunoprecipitated from cell lysates with anti-HA antibody, followed by immunoblotting using antibodies against HA tag, phospho-Ser/Thr, or Sec23. Lysates from cells expressing Sec16-AcGFP were used as the negative control (–). (B) Sec16-HA, Sec16$^{\Delta Np}$-HA, and Sec16$^{\Delta Cp}$-HA were immunoprecipitated, followed by immunoblotting as described in A. The right panels in A and B show quantifications of the band intensity of Sec23 relative to that of Sec16-HA in the immunoprecipitation (IP) fraction. The band intensity of Sec23 coimmunoprecipitated with Sec16-HA was set to 1. Error bars indicate the SD of three or more experiments.

whether Sec16 phosphorylation affects the interaction with Sec23. Both Sec16-HA and Sec16$^{\Delta NCp}$-HA exhibited coprecipitation of Sec23. However, an almost twofold higher level of Sec23 was coprecipitated with Sec16$^{\Delta NCp}$-HA compared with that with Sec16-HA (Figure 3A). Collectively, these results indicate that Sec16$^{\Delta NCp}$ is not indeed phosphorylated but can interact with Sec23 more efficiently than wild-type Sec16. Further coimmunoprecipitation experiments revealed that neither Sec16$^{\Delta Np}$-HA nor Sec16$^{\Delta Cp}$-HA showed remarkably increased interaction with Sec23 (Figure 3B), suggesting some redundancy of the Sec23-binding sites in the N- and C-terminal regions of Sec16.

Autophagy requires the N-terminal region of Sec16 but not its phosphorylation

We expressed Sec16 mutants in *sec16*Δ cells with Pgk1-GFP and examined autophagy by using Pgk1-GFP processing assay. When autophagy is induced under nitrogen starvation, cytoplasmic Pgk1-GFP is nonselectively engulfed along with other cytoplasmic materials within autophagosomes, and then delivered to the vacuole, where the GFP moiety is cleaved by vacuolar proteolysis. Because the cleaved GFP is relatively stable and detectable by immunoblotting, monitoring its level provides the degree of the autophagic activity (Welter *et al.*, 2010). After 2 h nitrogen starvation, both wild-type Sec16 and Sec16$^{\Delta 565N}$ exhibited GFP cleavage but the cleaved GFP level of Sec16$^{\Delta 565N}$ was lower than that of wild-type Sec16 (Figure 4, A and C), whereas wild-type Sec16 never raised cleaved GFP in *atg1*Δ cells. These results indicate that autophagy relies on the N-terminal region of Sec16, suggesting that Sec16 interaction with Sec31 in the N-terminal region is an essential process to potentiate COPII subunits to form both vesicles targeting to the Golgi and to autophagosomes at ERES. Another possibility is that this interaction is involved in the proper ERES formation and then maintains the contact between the ERES and the PAS to ensure the flow of lipids from the ER to autophagosomes. In this case, Sec16 might interact with Atg proteins localizing to the PAS through the N-terminal region, which directly maintains the ERES–PAS contact. Sec16 has been found to interact with Atg8 (Graef *et al.*, 2013). Future studies are needed to clarify the binding site and the role of their interaction in autophagy.

In contrast, each of the nonphosphorylatable mutants showed GFP cleavage at a level similar to the wild-type protein (Figure 4, B and C). These results indicate that in *S. cerevisiae*, Sec16 phosphorylation is dispensable for its function in not only ER export but also autophagy. Because Sec23 forms the stable complex with Sec24 paralogues (Hicke *et al.*, 1992; Roberg *et al.*, 1999; Kurihara *et al.*, 2000), however, our finding that Sec16$^{\Delta NCp}$ alters interaction with Sec23 may imply that Sec16 phosphorylation can influence its ability to interact with the complex of Sec23/Sec24 paralogues to regulate ER export of the specific cargo. This is in accord with the previous observation that the phosphorylation of Sec16A at Ser-846 modulates the interaction with Sec24C, a Sec24 isoform at ERES, and then drives the ER exit of Sec24C-specific cargoes (Joo *et al.*, 2016).

MATERIALS AND METHODS

Strains and media

Yeast strains used in this study are listed in Supplemental Table S1. All strains are isogenic to YPH500 (Sikorski and Hieter, 1989). To generate YTY343 and YTY397, PCR-based genomic integrations of GFP at the 3′ end of *MID2* and *PGK1* of YTY046 were carried out by using pFA6a-GFP-HIS3MX6 and pFA6a-GFP-hphMX6 as templates as described previously (Longtine *et al.*, 1998). Strains were grown at 30°C in YPD (2% polypeptone, 1% yeast extract, 2% glucose), SD (0.67% yeast nitrogen base without amino acids, 2% glucose) supplemented with appropriate nutrients, or SD-N (0.17% yeast nitrogen base without amino acids and ammonium sulfate, 2% glucose). Counterselection against *URA3*-containing plasmids was performed on SD plates containing 0.1% 5-fluoroorotic acid (5-FOA; Wako).

Plasmids

Plasmids pTYY42 (Sec16-AcGFP), pTYY48 (Sec16-HA), pTYY48-Δ565N (Sec16$^{\Delta 565N}$-HA), pTYY48-L1089P (Sec16^{L1089P}-HA), pFa6a-hphMX6, and pFA6a-GFP-HIS3MX6 were described previously (Longtine *et al.*, 1998; Hentges *et al.*, 2005; Yorimitsu and Sato, 2012). For pFA6a-GFP-hphMX6, a *Bam*HI/*Asc*I fragment containing GFP was cut from pFA6a-GFP-HIS3MX6 and inserted into the corresponding sites of pFa6a-hphMX6. For pTYY42-Δ565N (Sec16$^{\Delta 565N}$-AcGFP), a *Bam*HI/*Xho*I fragment containing 2xAcGFP was cut from

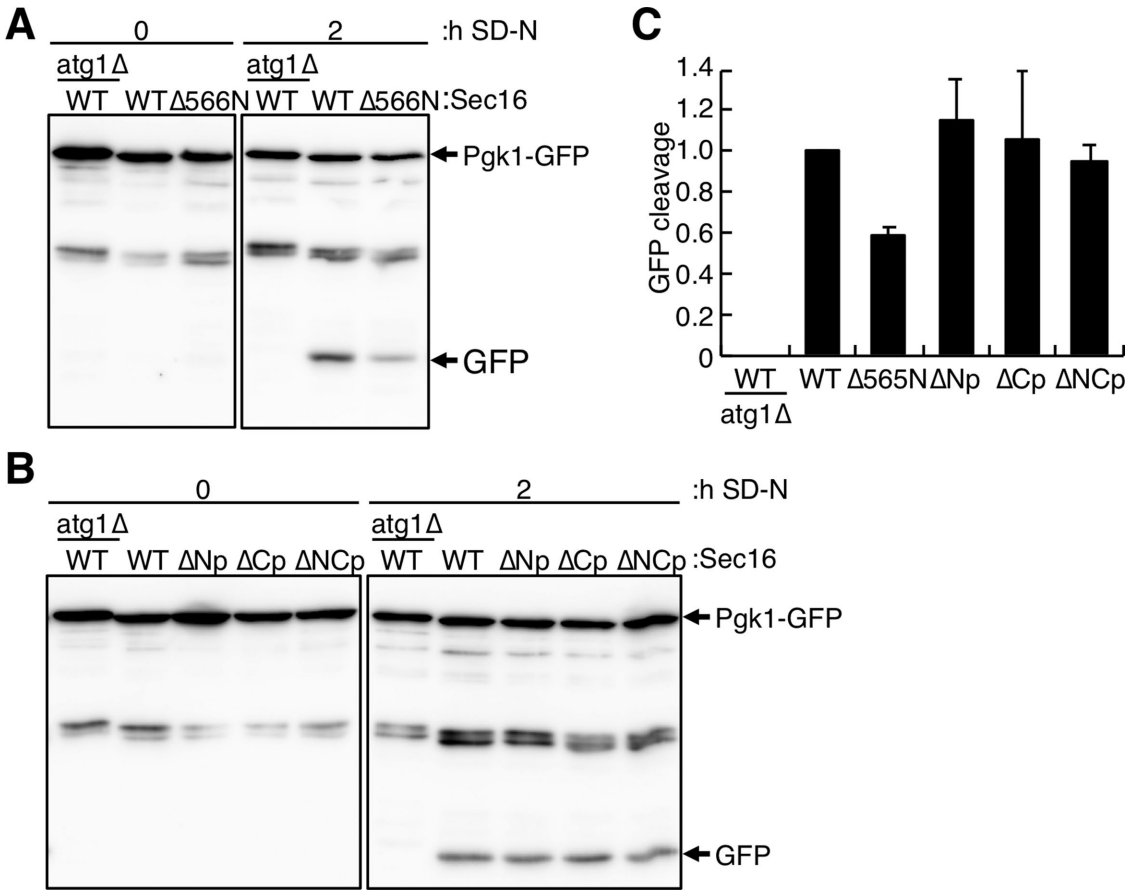

FIGURE 4: Autophagy is impaired by Sec16$^{\Delta 565N}$ mutant but not by nonphosphorylatable Sec16 mutants. Autophagy was monitored by Pgk1-GFP processing assays in *atg1Δ sec16Δ* cells expressing wild-type Sec16, and *sec16Δ* cells expressing wild-type Sec16 or Sec16$^{\Delta 565N}$ mutant (A) and the indicated Sec16 phosphomutants (B) after 2 h nitrogen starvation. (C) Quantification of the intensity of cleaved GFP relative to the total intensities of cleaved GFP and Pgk1-GFP. The GFP cleavage of wild-type Sec16 was set to 1. Error bars indicate the SD of three experiments.

pTYY42 and inserted into the corresponding sites of pTYY48-Δ565N. For pTYY48-ΔNp (Sec16$^{\Delta Np}$-HA) and pTYY48-ΔCp (Sec16$^{\Delta Cp}$-HA), DNA fragments coding Sec16$^{\Delta Np}$ and Sec16$^{\Delta Cp}$ were synthesized by gBlocks (IDT), and inserted into the *Nhe*I/*Hpa*I- and *Hpa*I/*Bam*HI-digested pTYY48, respectively, by using NEBuilder assembly kit (NEB). For pTYY48-ΔNCp (Sec16$^{\Delta NCp}$-HA), the *Sac*I/*Hpa*I-digested fragment from pTYY48-ΔNp was inserted into the corresponding sites of pTYY48-ΔCp. For pTYY56 (Sec16-mUkG1)-based plasmids, DNA fragment coding the yeast codon-optimized mUkG1 as shown previously (Kaishima *et al.*, 2016) was synthesized by Europhins Genomics and inserted into the *Bam*HI/*Xho*I-digested pTYY48, pTYY48-ΔNp, pTYY48-ΔCp, and pTYY48-ΔNCp.

Immunoprecipitation

YTY047, YTY049, YTY049$^{\Delta Np}$, YTY049$^{\Delta Cp}$, and YTY049$^{\Delta NCp}$ cells were grown to midlog phase, and 600 OD_{600} units of cells were collected. After being washed with water, cells were resuspended in lysis buffer (25 mM HEPES, pH 8.0, 100 mM NaCl, 1 mM EDTA, 5% glycerol) with 2× protease inhibitor cocktail (cOmplete, EDTA-free; Roche) and 2× phosphatase inhibitor cocktail (PhosSTOP, Sigma-Aldrich) and disrupted by vigorous vortexing with glass beads at 4°C. Lysates were solubilized on ice for 20 min by adding octylglucoside (Dojindo) to a final concentration of 4%. After unsolubilized materials were removed by centrifugation at 10,000 × *g* for 5 min at 4°C, the supernatant was transferred to a new tube and equal volume of lysis buffer supplemented with 3 µl of mouse anti-HA antibody (901514; Biolegend) was added. After 2 h incubation at 4°C, protein A-sepharose beads (20 µl; GE Healthcare) were added and incubated for 1 h at 4°C. The beads were washed three times with lysis buffer containing 1% β-octylglucoside, and the proteins were eluted by boiling in SDS sample buffer. The eluted proteins were resolved by SDS–PAGE, followed by immunoblotting with rabbit anti-HA (561; MBL), mouse anti-phospho-Ser/Thr (612548; BD Transduction Laboratories), and goat anti-Sec23 antibodies (sc-20195; Santa Cruz).

Pgk1-GFP processing assay

Autophagy was monitored by Pgk1-GFP processing assay as described previously (Welter *et al.*, 2010). Cells grown in YPD medium up to midlog phase were shifted to SD-N medium. After 2 h incubation, cell lysates were prepared by vigorous vortexing with glass beads in SDS–PAGE sample buffer and then subjected to SDS–PAGE, followed by immunoblotting with mouse anti-GFP antibody (66002-1-Ig; Proteintech).

Fluorescence microscopy

Cells grown to midlog phase were imaged with an Olympus IX71 microscope (Olympus) equipped with a CSU10 spinning-disk confocal scanner (Yokogawa Electric Corporation) as described previously

(Yorimitsu and Sato, 2012). Images were taken with an electron-multiplying charge-coupled device camera (iXon, DV897; Andor Technology, South Windsor, CT), and analyzed using Adobe Photoshop and ImageJ.

ACKNOWLEDGMENTS

We thank the National BioResource Project, Yeast Genetic Resource Center (NBRP/YGRC), for the plasmid (pFa6a-hphMX6) and the members of the Sato laboratory for helpful discussions. This work was supported in part by a Grant-in-Aid for Scientific Research from the Japanese Ministry of Education, Culture, Sports, Science and Technology (Grant no. 26840031 and Grant no. 18K06126 to T.Y., Grant no. 16K07340 and Grant no. 17KT0105 to K.S.) and by the Naito Foundation and the Takeda Science Foundation (K.S.).

REFERENCES

Albuquerque CP, Smolka MB, Payne SH, Bafna V, Eng J, Zhou H (2008). A multidimensional chromatography technology for in-depth phosphoproteome analysis. Mol Cell Proteomics 7, 1389–1396.

Antonny B, Madden D, Hamamoto S, Orci L, Schekman R (2001). Dynamics of the COPII coat with GTP and stable analogues. Nat Cell Biol 3, 531–537.

Barlowe CK, Miller EA (2013). Secretory protein biogenesis and traffic in the early secretory pathway. Genetics 193, 383–410.

Barlowe C, Schekman R (1993). *SEC12* encodes a guanine-nucleotide-exchange factor essential for transport vesicle budding from the ER. Nature 365, 347–349.

Belden WJ, Barlowe C (2001). Role of Erv29p in collecting soluble secretory proteins into ER-derived transport vesicles. Science 294, 1528–1531.

Bharucha N, Liu Y, Papanikou E, McMahon C, Esaki M, Jeffrey PD, Hughson FM, Glick BS (2013). Sec16 influences transitional ER sites by regulating rather than organizing COPII. Mol Biol Cell 24, 3406–3419.

Bi X, Corpina RA, Goldberg J (2002). Structure of the Sec23/24–Sar1 pre-budding complex of the COPII vesicle coat. Nature 419, 271–277.

Bi X, Mancias JD, Goldberg J (2007). Insights into COPII coat nucleation from the structure of Sec23•Sar1 complexed with the active fragment of Sec31. Dev Cell 13, 635–645.

Castillon GA, Watanabe R, Taylor M, Schwabe TME, Riezman H (2009). Concentration of GPI-anchored proteins upon ER exit in yeast. Traffic 10, 186–200.

Connerly PL, Esaki M, Montegna EA, Strongin DE, Levi S, Soderholm J, Glick BS (2005). Sec16 is a determinant of transitional ER organization. Curr Biol 15, 1439–1447.

Davis S, Wang J, Ferro-Novick S (2017). Crosstalk between the secretory and autophagy pathways regulates autophagosome formation. Dev Cell 41, 23–32.

Davis S, Wang J, Zhu M, Stahmer K, Lakshminarayan R, Ghassemian M, Jiang Y, Miller EA, Ferro-Novick S (2016). Sec24 phosphorylation regulates autophagosome abundance during nutrient deprivation. eLife 5, e21167.

Espenshade P, Gimeno RE, Holzmacher E, Teung P, Kaiser CA (1995). Yeast *SEC16* gene encodes a multidomain vesicle coat protein that interacts with Sec23p. J Cell Biol 131, 311–324.

Farhan H, Wendeler MW, Mitrovic S, Fava E, Silberberg Y, Sharan R, Zerial M, Hauri HP (2010). MAPK signaling to the early secretory pathway revealed by kinase/phosphatase functional screening. J Cell Biol 189, 997–1011.

Feng Y, He D, Yao Z, Klionsky DJ (2014). The machinery of macroautophagy. Cell Res 24, 24–41.

Gan W, Zhang C, Siu KY, Satoh A, Tanner JA, Yu S (2017). ULK1 phosphorylates Sec23A and mediates autophagy-induced inhibition of ER-to-Golgi traffic. BMC Cell Biol 18, 22.

Gimeno RE, Espenshade P, Kaiser CA (1995). *SED4* encodes a yeast endoplasmic reticulum protein that binds Sec16p and participates in vesicle formation. J Cell Biol 131, 325–338.

Graef M, Friedman JR, Graham C, Babu M, Nunnari J (2013). ER exit sites are physical and functional core autophagosome biogenesis components. Mol Biol Cell 24, 2918–2931.

Hentges P, Van Driessche B, Tafforeau L, Vandenhaute J, Carr AM (2005). Three novel antibiotic marker cassettes for gene disruption and marker switching in *Schizosaccharomyces pombe*. Yeast 22, 1013–1019.

Hicke L, Yoshihisa T, Schekman R (1992). Sec23p and a novel 105-kDa protein function as a multimeric complex to promote vesicle budding and protein transport from the endoplasmic reticulum. Mol Biol Cell 3, 667–676.

Holt LJ, Tuch BB, Villen J, Johnson AD, Gygi SP, Morgan DO (2009). Global analysis of Cdk1 substrate phosphorylation sites provides insights into evolution. Science 325, 1682–1686.

Iesmantavicius V, Weinert BT, Choudhary C (2014). Convergence of ubiquitylation and phosphorylation signaling in rapamycin-treated yeast cells. Mol Cell Proteomics 13, 1979–1992.

Ishihara N, Hamasaki M, Yokota S, Suzuki K, Kamada Y, Kihara A, Yoshimori T, Noda T, Ohsumi Y (2001). Autophagosome requires specific early Sec proteins for its formation and NSF/SNARE for vacuolar fusion. Mol Biol Cell 12, 3690–3702.

Iwasaki H, Yorimitsu T, Sato K (2015). Distribution of Sec24 isoforms to each ER exit site is dynamically regulated in *Saccharomyces cerevisiae*. FEBS Lett 589, 1234–1239.

Iwasaki H, Yorimitsu T, Sato K (2017). Microscopy analysis of reconstituted COPII coat polymerization and Sec16 dynamics. J Cell Sci 130, 2893–2902.

Joo JH, Wang B, Frankel E, Ge L, Xu L, Iyengar R, Li-Harms X, Wright C, Shaw TI, Lindsten T, *et al*. (2016). The noncanonical role of ULK/ATG1 in ER-to-Golgi trafficking is essential for cellular homeostasis. Mol Cell 62, 491–506.

Kaishima M, Ishii J, Matsuno T, Fukuda N, Kondo A (2016). Expression of varied GFPs in *Saccharomyces cerevisiae*: codon optimization yields stronger than expected expression and fluorescence intensity. Sci Rep 6, 35932.

Kotani T, Kirisako H, Koizumi M, Ohsumi Y, Nakatogawa H (2018). The Atg2-Atg18 complex tethers pre-autophagosomal membranes to the endoplasmic reticulum for autophagosome formation. Proc Natl Acad Sci USA 115, 10363–10368.

Kung LF, Pagant S, Futai E, D'Arcangelo JG, Buchanan R, Dittmar JC, Reid RJ, Rothstein R, Hamamoto S, Snapp EL, *et al*. (2012). Sec24p and Sec16p cooperate to regulate the GTP cycle of the COPII coat. EMBO J 31, 1014–1027.

Kurihara T, Hamamoto S, Gimeno RE, Kaiser CA, Schekman R, Yoshihisa T (2000). Sec24p and Iss1p function interchangeably in transport vesicle formation from the endoplasmic reticulum in *Saccharomyces cerevisiae*. Mol Biol Cell 11, 983–998.

Lemus L, Ribas JL, Sikorska N, Goder V (2016). An ER-localized SNARE protein is exported in specific COPII vesicles for autophagosome biogenesis. Cell Rep 14, 1710–1722.

Longtine MS, McKenzie A 3rd, Demarini DJ, Shah NG, Wach A, Brachat A, Philippsen P, Pringle JR (1998). Additional modules for versatile and economical PCR-based gene deletion and modification in *Saccharomyces cerevisiae*. Yeast 14, 953–961.

Lord C, Bhandari D, Menon S, Ghassemian M, Nycz D, Hay J, Ghosh P, Ferro-Novick S (2011). Sequential interactions with Sec23 control the direction of vesicle traffic. Nature 473, 181–186.

Lord C, Ferro-Novick S, Miller EA (2013). The highly conserved COPII coat complex sorts cargo from the endoplasmic reticulum and targets it to the Golgi. Cold Spring Harb Perspect Biol 5, a013367.

Matsuoka K, Orci L, Amherdt M, Bednarek SY, Hamamoto S, Schekman R, Yeung T (1998). COPII-coated vesicle formation reconstituted with purified coat proteins and chemically defined liposomes. Cell 93, 263–275.

Miller E, Antonny B, Hamamoto S, Schekman R (2002). Cargo selection into COPII vesicles is driven by the Sec24p subunit. EMBO J 21, 6105–6113.

Miller EA, Beilharz TH, Malkus PN, Lee MC, Hamamoto S, Orci L, Schekman R (2003). Multiple cargo binding sites on the COPII subunit Sec24p ensure capture of diverse membrane proteins into transport vesicles. Cell 114, 497–509.

Nakano A, Muramatsu M (1989). A novel GTP-binding protein, Sar1p, is involved in transport from the endoplasmic reticulum to the Golgi apparatus. J Cell Biol 109, 2677–2691.

Nakatogawa H, Suzuki K, Kamada Y, Ohsumi Y (2009). Dynamics and diversity in autophagy mechanisms: lessons from yeast. Nat Rev Mol Cell Biol 10, 458–467.

Ono T, Suzuki T, Anraku Y, Iida H (1994). The *MID2* gene encodes a putative integral membrane protein with a Ca^{2+}-binding domain and shows mating pheromone-stimulated expression in *Saccharomyces cerevisiae*. Gene 151, 203–208.

Pietrosemoli N, Pancsa R, Tompa P (2013). Structural disorder provides increased adaptability for vesicle trafficking pathways. PLoS Comput Biol 9, e1003144.
Roberg KJ, Crotwell M, Espenshade P, Gimeno R, Kaiser CA (1999). LST1 is a *SEC24* homologue used for selective export of the plasma membrane ATPase from the endoplasmic reticulum. J Cell Biol 145, 659–672.
Shaywitz DA, Espenshade PJ, Gimeno RE, Kaiser CA (1997). COPII subunit interactions in the assembly of the vesicle coat. J Biol Chem 272, 25413–25416.
Shima T, Kirisako H, Nakatogawa H (2019). COPII vesicles contribute to autophagosomal membranes. J Cell Biol 218, 1503–1510.
Shindiapina P, Barlowe C (2010). Requirements for transitional endoplasmic reticulum site structure and function in *Saccharomyces cerevisiae*. Mol Biol Cell 21, 1530–1545.
Sikorski RS, Hieter P (1989). A system of shuttle vectors and yeast host strains designed for efficient manipulation of DNA in *Saccharomyces cerevisiae*. Genetics 122, 19–27.
Sprangers J, Rabouille C (2015). *SEC16* in COPII coat dynamics at ER exit sites. Biochem Soc Trans 43, 97–103.
Suzuki K, Akioka M, Kondo-Kakuta C, Yamamoto H, Ohsumi Y (2013). Fine mapping of autophagy-related proteins during autophagosome formation in *Saccharomyces cerevisiae*. J Cell Sci 126, 2534–2544.
Swaney DL, Beltrao P, Starita L, Guo A, Rush J, Fields S, Krogan NJ, Villen J (2013). Global analysis of phosphorylation and ubiquitylation cross-talk in protein degradation. Nat Methods 10, 676–682.
Tabata KV, Sato K, Ide T, Nishizaka T, Nakano A, Noji H (2009). Visualization of cargo concentration by COPII minimal machinery in a planar lipid membrane. EMBO J 28, 3279–3289.
Welter E, Thumm M, Krick R (2010). Quantification of nonselective bulk autophagy in *S. cerevisiae* using Pgk1-GFP. Autophagy 6, 794–797.
Whittle JRR, Schwartz TU (2010). Structure of the Sec13–Sec16 edge element, a template for assembly of the COPII vesicle coat. J Cell Biol 190, 347–361.
Yorimitsu T, Sato K (2012). Insights into structural and regulatory roles of Sec16 in COPII vesicle formation at ER exit sites. Mol Biol Cell 23, 2930–2942.
Yoshihisa T, Barlowe C, Schekman R (1993). Requirement for a GTPase-activating protein in vesicle budding from the endoplasmic reticulum. Science 259, 1466–1468.
Zacharogianni M, Kondylis V, Tang Y, Farhan H, Xanthakis D, Fuchs F, Boutros M, Rabouille C (2011). ERK7 is a negative regulator of protein secretion in response to amino-acid starvation by modulating Sec16 membrane association. EMBO J 30, 3684-3700.
Zahoor M, Farhan H (2018). Crosstalk of autophagy and the secretory pathway and its role in diseases. Int Rev Cell Mol Biol 337, 153–184.